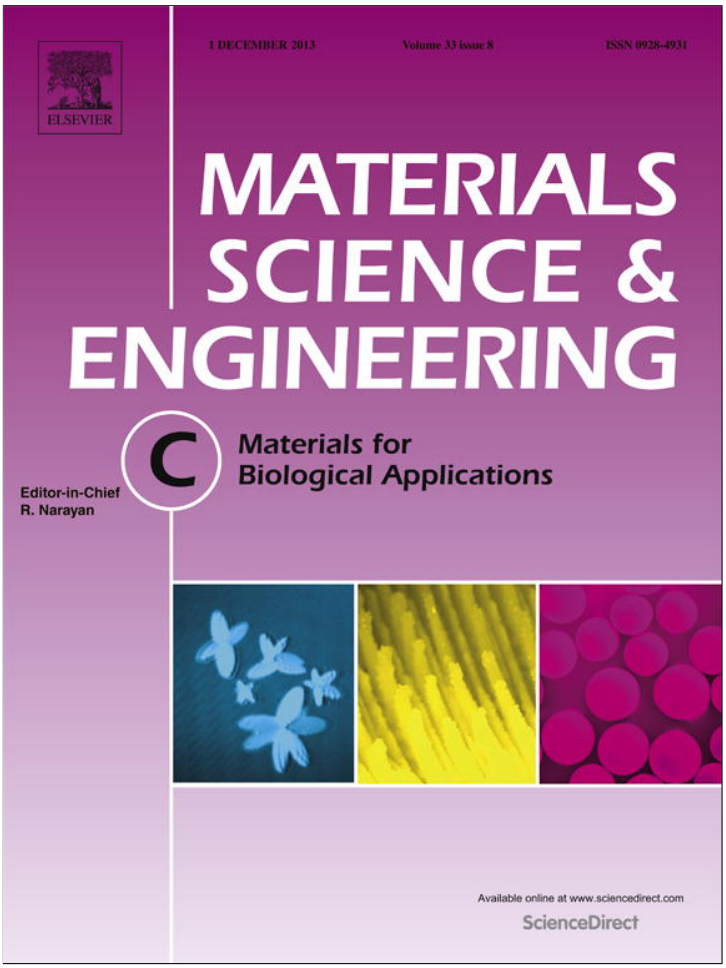

Materials Science and Engineering C 33 (2013) 5079–5083

Contents lists available at ScienceDirect

Materials Science and Engineering C

journal homepage: www.elsevier.com/locate/msec

DNA adsorption characteristics of hollow spherule allophane nano-particles

Yoko Matsuura [a], Fumitoshi Iyoda [a], Shuichi Arakawa [a], Baiju John [a], Masami Okamoto [a,*], Hidetomo Hayashi [b]

[a] Advanced Polymeric Nanostructured Materials Engineering, Graduate School of Engineering Toyota Technological Institute, 2-12-1 Hisakata, Tempaku, Nagoya 468-8511, Japan
[b] New Product Development Center, Tsuchiya Co., Ltd., 22-4 Higashinamikita, Yamamachi, Chiryu 472-0006, Japan

ARTICLE INFO

Article history:
Received 11 January 2013
Received in revised form 24 July 2013
Accepted 29 August 2013
Available online 7 September 2013

Keywords:
Natural allophane
Single-stranded DNA
Adsorption
Clustered particles

ABSTRACT

To understand the propensity of natural allophane to adsorb the DNA molecules, the adsorption characteristics were assessed against natural allophane (AK70), using single-stranded DNA (ss-DNA) and adenosine 5′-monophosphate (5′-AMP) as a reference molecule. The adsorption capacity of ss-DNA on AK70 exhibited one order of magnitude lower value as compared with that of 5′-AMP. The adsorption capacity of ss-DNA decreased with increasing pH due to the interaction generated between phosphate groups of ss-DNA and functional Al–OH groups on the wall perforations through deprotonating, associated with higher energy barrier for the adsorption of ss-DNA. The adsorption morphologies consisting of the individual ss-DNA with mono-layer coverage of the clustered allophane particle were observed successfully through transmission electron microscopy analysis.

1. Introduction

Clay minerals are found in abundance on the Earth today. In 1949 Bernal suggested five key points of clay minerals in the origins of life [1]. The advantageous features of clays are: (i) their ordered structure, (ii) their large adsorption capacity, (iii) their shielding against sunlight, (iv) their ability to concentrate organic chemicals, and (v) their ability to serve as polymerization templates. Most clay minerals are formed by aqueous alternation of silicate mineral [2]. Liquid water is permanently present on the surface of the Earth; clay minerals accumulate and disperse in the water reservoir. According to the seminal hypothesis of Bernal [1], many prebiotic scenarios including clay minerals were described and many prebiotic experiments were conducted using clays. Montmorillonite (MMT) has been found to catalyze a number of organic reactions on the primitive Earth [3]. The formation of oligomer of ribonucleic acid (RNA) that contains monomer units from 2 to 50 is catalyzed by MMT. The oligomer of this length is formed because this catalyst controls the structure of the oligomers synthesized and does not generate all possible isomers. Evidence of sequence-, regio- and homochiral selectivity in these oligomers has been obtained [4].

The ribozyme, which plays important roles both information molecules and enzymes, has been made at the very beginning of the origin of life in the RNA world hypothesis [5]. However, ultraviolet degrade extracellular RNA and deoxyribonucleic acid (DNA) molecules produced through this hypothesis. For the protection of DNA, the adsorption of DNA molecules on clay particles may be significant. It shall give insights into the origin of life and subsequent survival of the same on this planet. Moreover, the persistent ability of the DNA molecules could transform competent cells when the DNA molecules bound to clay minerals and humic acids [6].

Allophane is a short-range-order clay mineral and occurs in some soils derived from volcanic ejecta and is able to protect the extracellular DNA and RNA molecules from ultraviolet light. The primary particle of the allophane is a hollow spherule with an outer diameter of 3.5–5.0 nm and a wall of about 0.6–1.0 nm thick, which has perforations as shown in Fig. 1 [7,8]. The surface area of allophane is as high as ~1000 m^2/g, which is often larger than activated carbon. In addition to this large surface area, the $(OH)Al(OH_2)$ groups exposed on the wall perforations are the source of the pH-dependent charge characteristics of allophane.

It is possible to investigate the origin of the living organisms and environments of the ancient earth by researching DNA in allophane clusters of the soil. The adsorption behavior of DNA or RNA molecules on allophane particles has been investigated. Many researchers have discussed the adsorption by using the Langmuir adsorption equation without deep insights into the morphological feature [9–11]. For this reason, the mechanism of DNA molecule adsorption and its sustenance (morphology) in clustered allophane particles is not fully revealed yet.

We also examined the morphology observation to provide insight into the adsorption structure and characteristics of ss-DNA by the allophane particles, which is the first time of the real images obtained from a microscopic experiment.

In our previous paper [8], we have examined the adsorption characteristics of adenosine 5′-monophosphate (5′-AMP) and adenine by natural allophane. The adsorption capacity of the natural allophane for 5′-AMP was three times higher than that for adenine. Therefore, the

* Corresponding author. Tel.: +81 528091861; fax: +81 528091864.
E-mail address: okamoto@toyota-ti.ac.jp (M. Okamoto).

0928-4931/$ – see front matter © 2013 Elsevier B.V. All rights reserved.
http://dx.doi.org/10.1016/j.msec.2013.08.040

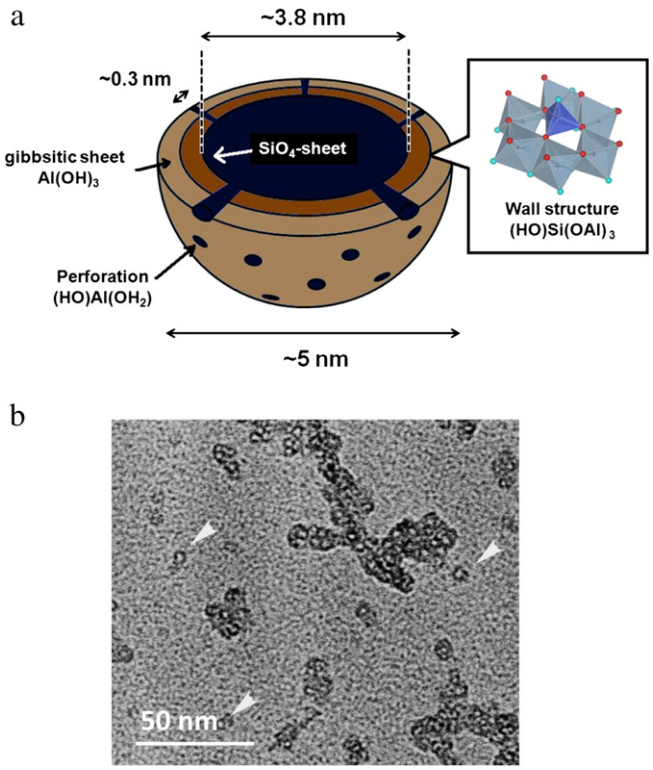

Fig. 1. (a) Schematic representation of allophane structure. The overall size of a single allophane particle is ~5 nm. The pore-size distribution of AK70 shows a peak at ~1.9 nm. (b) High resolution TEM image of clustered particles of AK70, rather than singular particles. Arrows indicate single unit particles of allophane.

adenine without phosphate group has some possibility of the interaction between allophane particles.

The single-stranded DNA (ss-DNA) molecules are one of the most important adsorbates of biological polymers on allophane particles. However, the research on the adsorption of ss-DNA on the allophane particles is at its infancy.

The objective of this study is the analysis of the propensity and morphology of the natural allopane to adsorb the ss-DNA molecules. The adsorption characteristics were assessed against a natural allophane, using ss-DNA and 5′-AMP as a reference molecule, which is a nucleotide found in RNA and widely studied in the biological systems. Knowledge of such a comparison between ss-DNA and 5′-AMP adsorption on natural allophane clusters should also be useful in assessing how the ss-DNA molecules control the adsorption properties.

2. Experimental section

2.1. Materials

The allophane sample was provided by Shinagawa Chemicals Ltd. and designated as AK70. The overall size of a single allophane particle is ~5 nm with a surface area of 250 m^2g^{-1}, which was estimated by the *t*-method [12] (Fig. 1). The functional groups (HO)Al(OH_2) exposed on the wall perforations play a significant role in the adsorption process [13]. The Si/Al ratio (=0.58) of the sample was determined by dissolution in acidic ammonium oxalate solution [8,14].

The ss-DNA taken from calf thymus was purchased from Sigma-Aldrich (D8899; $M_w = 1.64 \times 10^7$ Da, 5×10^4 base). The guanine–cytosine (G–C) content was reported to be 41.9 mol%. 5′-AMP was purchased from Wako Pure Chemicals, Japan. HCl, NaCl and NaOH (Nacalai Tesque) were not further purified for use.

2.2. Adsorption experiments

AK70 was dispersed in aqueous adsorbate solutions. 5 mg of AK70 with 0.1-2.0 mM aqueous solutions of 5′-AMP was mixed. In the case of ss-DNA solutions, 5 mg of AK70 with 0.1–1.0 nM aqueous solutions for ss-DNA was mixed. In addition 250 μl of 2.0 M NaCl solution was added in each solution and the desired pH that ranged from 3.0 to 9.0 was adjusted using dilute HCl and NaOH. Millipore Milli Q ultrapure (18 MΩ cm, total organic carbon (TOC) < 20 ppb, Merck Millipore Co., Japan) water through dialysis membrane was used in all experiment. The mixtures were shaken well for 60 h in the temperature range of 5–35 °C. 60 h was fixed as the equilibrium time throughout this study because adsorption uptake approached the constant value. Thereafter the tubes were centrifuged at a speed of 6000 rpm for 20 min. The TOC and total nitrogen (TN) of supernatant solutions were measured by using combustion method with a set temperature of 800 °C after four point calibration using an instrument (multi N/C 2100S Analytik Jana) [8].

The amount of adsorption (Q_{ads}) increases with the equilibrium concentration of adsorbates ($[A]_e$). The adsorption isotherms of 5′-AMP and ss-DNA on natural allophane (Fig. 2) were fitted by the Freundlich equation ($r^2 \geq 0.95$),

$$Q_{ads} = K_f [A]_e^{1/N} \quad (1)$$

where K_f is the relative adsorption capacity of the adsorbent and N is the adsorption intensity, which describes the shape of the isotherm. The adsorption isotherms exhibited a marked curvature, with slopes ($1/N$) significantly < 1.0, indicating a convex up curvature, or L-type isotherm. The slope of the isotherms steadily decreased with increasing adsorptive concentration because the vacant sites became less accessible with the progressive covering of the adsorbent surface [15].

2.3. Characterization

Pore-size distribution was measured by the Cranston–Inkley method [16] using a nitrogen adsorption isotherm (BELSORP-mini, Bel Japan, Inc.). The adsorption isotherm of AK70 exhibited type IV nitrogen isotherm (IUPAC classification). The surface area was estimated by *t*-method [12].

The adsorption morphology of the ss-DNA on the allophane nanoparticles in the sediment at pH 7.0 was observed through transmission electron microscopy (TEM) using the Dual Vision camera

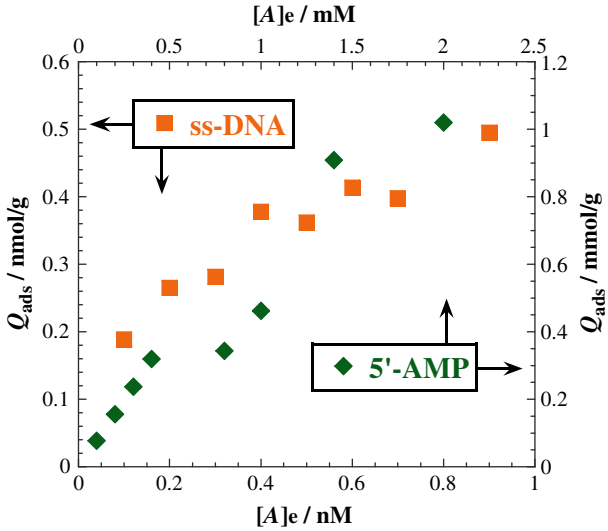

Fig. 2. Adsorption isotherms of 5′-AMP and ss-DNA on AK70 at 25 °C in the pH 6.5.

from Gatan on a TEM (JEM-1230, Jeol Co.) operated at an accelerating voltage of 120 kV. The sediment was prepared on copper grids with 300 mesh size, and then water was removed by placing filter paper at the edge of the grids.

The surface charge characteristics of AK70 were determined by electrophoresis (Zetasizer Nano ZS, Malvern Instruments, UK) by the technique of laser Doppler anemometry. The method involved washing AK70 several times with water and adjusting the pH of the suspension in the range of 3.0–9.0 using dilute HCl and NaOH. All measurements were performed for three replicates and averaged to get the final value.

Fourier Transform Infrared (FTIR) spectra were collected at 1 cm^{-1} nominal resolution using a FTIR spectrometer (FT-730, Horiba Ltd.) equipped with ZnSe mull omni-cell window (GS01834, Specac Co., UK) in transmission mode. The spectra were obtained by averaging 32 scans with a mean collection length of 1 s per spectrum. The background spectra used for reduction were collected with sample. By subtracting the spectrum of AK70 from the consecutive spectra of ss-DNA/AK70 mixtures, a difference spectrum was processed by software.

3. Results and discussion

Fig. 2 shows the adsorption isotherms of 5′-AMP and ss-DNA at 25 °C in the pH 6.5. The isotherms were fitted by the Freundlich equation with r^2 values ≥0.95, and the values are listed in Table 1. The adsorption of 5′-AMP by AK70 shows five order of magnitude higher value of K_f (=0.157 mol/g mol/$l^{-1/N}$) than that of the ss-DNA (K_f = 2.83 × 10^{-6} mol/g mol/$l^{-1/N}$). The adsorption capacities in mass of adsorbates per unit mass of AK70 are 0.46 and 0.045 g/g g/$l^{-1/N}$ for 5′-AMP and for ss-DNA, respectively. That is, the adsorption capacity of ss-DNA on AK70 exhibits one order of magnitude lower value as compared with that of 5′-AMP. The adsorptions of both 5′-AMP and ss-DNA are facilitated by the interaction between the phosphate groups and the Al–OH groups on the wall perforations and the interstitial spaces of the cluster of allophanes. This involves the formation of inner-sphere complex through a ligand-exchange reaction between Al–OH and phosphate groups ($(HO)_2OP{=}O$ for 5′-AMP and PO_2^- for ss-DNA) [8,17]. However, the ss-DNA chains are macromolecules, which hindered the adsorption of the same on the allophanes as compared to the small and compact 5′-AMP molecules.

The adsorption isotherms of ss-DNA on AK70 at three different pHs were examined to clarify the interaction generated between the phosphate groups and the Al–OH groups. The surface charge characteristics of allophane are very different from those of MMT. Allophane has a variable or pH-dependent surface charge, because the $(HO)Al(OH_2)$ groups, exposed at surface defect sites, can either acquire or lose protons depending on the pH of the ambient solution. They become $^{+}(OH_2)Al(OH_2)$ by acquiring protons on the acid side of the point of zero charge (PZC), and become $(OH)Al(OH)^{-}$ by losing protons on the alkaline side. The results of the zeta potential measurements of AK70 are shown in Table 1. The PZC of AK70 was (pH) 7.3. In the pH range of 5–7, both positively and negatively charged species are present on the surface of allophane particle. They are able to adsorb cations and anions at the same time [13].

Table 1
Adsorption parameters of 5′-AMP and ss-DNA and zeta potential of AK70.

Adsorbents	Adsorbates	pH –	K_f/ mol/g mol/$l^{-1/N}$	N –	r^{2a} –	E_a/ kJ/mol	Zeta potential/ mV
AK70	5′-AMP	6.5	0.157	1.23	0.95*	–	+14.8
	ss-DNA	6.5	2.83 × 10^{-6}	2.39	0.96	–	+14.8
		3.0	4.53 × 10^{-3}	1.38	0.99	24.3	+39.0
		7.0	1.59 × 10^{-5}	2.04	0.98	32.0	+6.6
		9.0	3.08 × 10^{-7}	2.97	0.97	59.1	−31.2

[a] The values are calculated by a log–log linear regression.
* Significant at p = 0.05 level.

The adsorption capacity of ss-DNA decreases with increasing pH (Table 1). The functional Al–OH groups exposed on the wall perforations of allophane shall be protonated with a lower pH value of the ss-DNA medium. The phosphate groups of ss-DNA possess a negative charge (PO_2^-) [18] that bind directly to the protonated Al–OH groups through an electrostatic interaction leading to an increased adsorption. On the contrary, the Al–OH groups possess a negative charge through deprotonation with an increase in pH of the medium. Thus the adsorption ability of allophanes is highly depended on the interactions of phosphate and Al–OH groups through protonation and deprotonation with a varying pH.

The frequencies and the vibrational assignments for the DNA with B-form are reported in the literature [19]. The sensitive bands at 1226 cm^{-1} (asymmetric stretching mode of PO_2^- groups: $\nu_{as}(PO_2^-)$), 1086 cm^{-1} (symmetric stretching mode: $\nu_s(PO_2^-)$) and 1054 cm^{-1} (stretching of ribose ν(C–C)) of the phosphodiester–deoxyribose backbone provide valuable information to understand the interaction generated between ss-DNA backbone and allophane surfaces. By subtracting the spectrum of AK70 from the consecutive spectra of ss-DNA/AK70 hydrogel-like mixture recovered from the sediment with ~40 wt.% ss-DNA at pH 7.0, a difference spectrum was obtained (Fig. 3). The presence of the sensitive bands in the difference spectrum is also confirmed. We notice that $\nu_{as}(PO_2^-)$ band shifts to the lower frequency side from 1226 to 1220 cm^{-1}. In contrast, the variation of $\nu_s(PO_2^-)$ exhibits nearly constant. The formation of the interaction between PO_2^- groups of ss-DAN and AK70 surfaces was suggested.

The activation energy was assessed by the temperature dependence of the adsorption behavior of ss-DNA at different pHs. Now, assuming that the Q_{ads} value for long time (~60 h) is of Arrhenius-type, Q_{ads} is given as

$$Q_{ads} \sim \exp(E_a/RT) \quad (2)$$

where E_a is the activation energy for the adsorption, and RT is the thermal energy. To confirm our consideration, in Fig. 4 we constructed an Arrhenius plot of Q_{ads} versus $1/T$. The slope reflects the E_a value, indicating an increase with increasing pH of the medium (Table 1). This feature is superficially similar to the change in K_f value as shown in Table 1. A significant decrease in K_f is correlated with E_a associated with higher

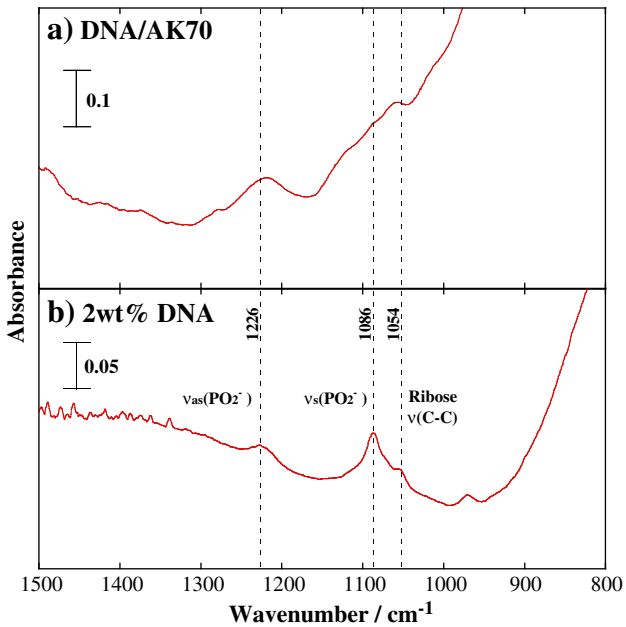

Fig. 3. FTIR spectra of (a) difference spectra of ss-DNA/AK70 mixture recovered from the sediment with ~40 wt.% ss-DNA and (b) 2 wt.% ss-DNA aqueous solution in the region of 800–1500 cm^{-1}.

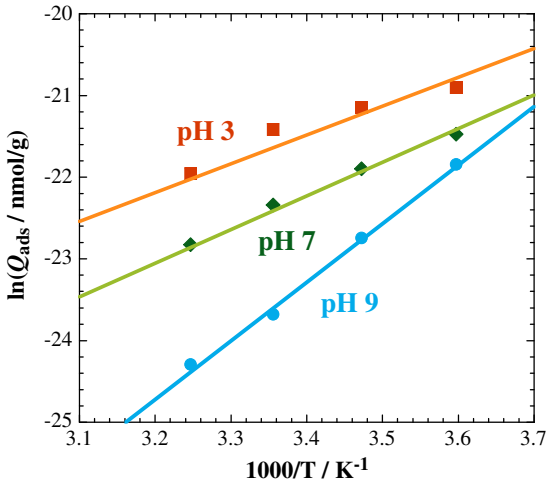

Fig. 4. Temperature dependence of adsorption capacity of ss-DNA on AK70 at different pHs.

energy barrier for the adsorption of ss-DNA, which leads to an inverse in adsorption.

TEM offers a qualitative understanding of the adsorption structure through direct visualization. Fig. 5 shows the results of TEM bright field images. Before adsorption on AK70, the ss-DNA exhibits a helical configuration with a width of ~10 nm (Fig. 5a). A single ss-DNA molecule isolated from entangled molecules is highly flexible and continuous over lengths of several micrometers. After the adsorption of ss-DNA molecules on AK70 at pH 7.0, typically discrete ss-DNA, ~300 nm in length, accompanied with clustered allophane particle with a width of ~20 nm on the surface of ss-DNA molecule is observed (Fig. 5b), which possibly represented individual ss-DNA molecule adsorbed on AK70 surface. Interconnected discrete chains associated with condensation of the allophane clusters could also be observed (Fig. 5c). The interstitial spaces of the cluster may play an important role in the adsorption of ss-DNA molecules. The clustered allophane particles may lead to the formation of network structure as well as bundled thicker strand. Significantly, the allophane cluster is covered over single ss-DNA molecule associated with surface binding. This could be routinely imaged (Fig. 5d). The ss-DNA is imaged as a hairpin tube like double-stranded DNA [20]. The individual ss-DNA with monolayer coverage of the cluster may be ascribed to the formation of the interaction between PO_2^- groups of ss-DNA and AK70 surfaces as revealed by FTIR analysis.

4. Conclusions

In this study, we have demonstrated that the relative adsorption capacities of ss-DNA on AK70 exhibit one order of magnitude lower value as compared with that of 5′-AMP. The adsorption of ss-DNA was facilitated by the interaction between the phosphate groups with the Al–OH groups on the wall perforations and the interstitial spaces of the clustered particles of allophane. The adsorption capacity of ss-DNA (K_f) decreases with increasing pH due to the interaction generated between phosphate groups of ss-DNA and functional Al–OH groups through deprotonating, associated with higher energy barrier (E_a) for the adsorption of ss-DNA, which leads to an inverse in adsorption. The adsorption morphologies consisting of the individual ss-DNA with mono-layer coverage of the clustered allophane particle were successfully observed through TEM analysis.

Author contributions

The manuscript was written through contributions of all authors. All authors have given approval to the final version of the manuscript.

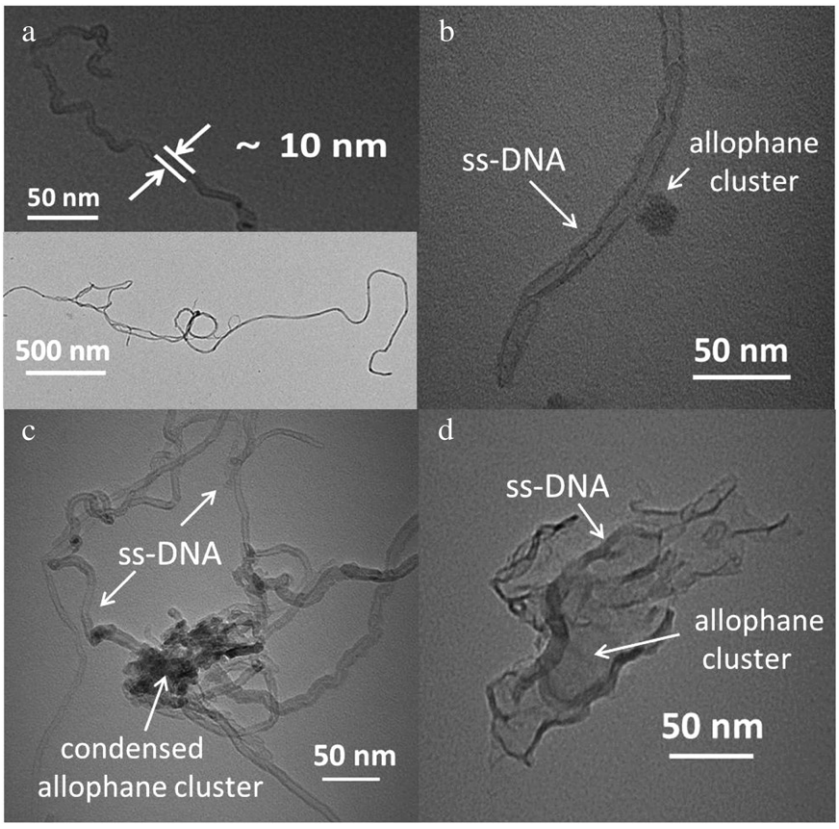

Fig. 5. TEM images showing (a) single ss-DNA molecule (inset shows lower magnification image), (b) discrete ss-DNA accompanied with the allophane cluster, (c) interconnected discrete chains associated with condensation of the allophane clusters, and (d) individual ss-DNA with mono-layer coverage of the cluster.

Conflict of interest

The authors declare no competing financial interest.

Acknowledgments

This work was supported by the Strategic Research Infrastructure Project of the Ministry of Education, Sports, Science and Technology, Japan (2010–2014).

References

[1] J.D. Bernal, Proc. Phys. Soc. Lond. Sel. A 62 (1949) 537–558.
[2] E. Galán, Genesis of clay minerals, in: F. Bergaya, B.K.G. Theng, G. Lagaly (Eds.), Handbook of Clay Science, Elsevier, Amsterdam, 2006, pp. 1129–1162.
[3] M.D. Nikalje, P. Puhukan, A. Sudalai, Org. Prep. Proced. Int. 32 (2000) 1–40.
[4] J.P. Ferris, Phil. Trans. R. Soc. B 361 (2006) 1777–1786.
[5] W. Gilbert, Nature 319 (1986) 618.
[6] G. Stotzky, J. Environ. Qual. 29 (2000) 691–705.
[7] M.F. Brigatti, E. Galan, B.K.G. Theng, Structures and mineralogy of clay minerals, in: F. Bergaya, B.K.G. Theng, G. Lagaly (Eds.), Handbook of Clay Science, Elsevier, Amsterdam, 2006, pp. 19–86.
[8] F. Iyoda, S. Hayashi, S. Arakawa, M. Okamoto, Appl. Clay Sci. 56 (2012) 77–83.
[9] K. Saeki, M. Sakai, S.I. Wada, Appl. Clay Sci. 50 (2010) 493–497.
[10] D.H. Taylor, A.T. Wilson, Clays Clay Miner. 27 (1979) 261–268.
[11] H.J. Cleaves II, E. Crapster-Pregont, C.M. Jonsson, C.L. Jonsson, D.A. Sverjensky, R.A. Hazen, Chemosphere 83 (2011) 1560–1567.
[12] B.C. Lippens, J.H. de Boer, J. Catal. 4 (1965) 319–323.
[13] G. Yuan, S.I. Wada, Allophane and imogolite nanoparticles in soil and their environmental applications, in: A.S. Barnard, H.B. Guo (Eds.), Nature's Nanostructures, Pan Stanford Publishing Pte Ltd., 2012, pp. 485–508.
[14] B.K.G. Theng, M. Russell, G.J. Churchman, R.L. Parfitt, Clays Clay Miner. 30 (1982) 143–149.
[15] C.H. Giles, T.H. MacEwan, S.N. Nakhwa, D. Smith, J. Chem. Soc. 148 (1960) 3973–3993.
[16] R.W. Cranston, F.A. Inkley, Adv. Catal. 9 (1957) 143–154.
[17] H. Hashizume, B.K.G. Theng, Clays Clay Miner. 55 (2007) 599–605.
[18] A. Taki, B. John, S. Arakawa, M. Okamoto, Eur. Polym. J. 49 (2013) 923–931.
[19] S.H. Brewer, S.J. Anthireya, S.E. Lappi, D.L. Drapcho, S. Franzen, Langmuir 18 (2002) 4460–4464.
[20] P.R. O'Neill, K. Young, D. Schiffels, D.K. Fygenson, Nano lett. 12 (2012) 5464–5469.